https://doi.org/10.5194/egusphere-2026-2385
Preprint. Discussion started: 28 July 2026

A flexible open-source modular framework for ecohydrological modeling: Application and validation of GEOSPACE-1D

Concetta D'Amato[1,2,3], Paolo Benettin[4], Andrea Rinaldo[5], and Riccardo Rigon[2,3]

[1]Laboratory of Catchment Hydrology and Geomorphology, École Polytechnique Fédérale de Lausanne, Sion, Switzerland
[2]Center Agriculture Food Environment, Università di Trento, Trento, Italy
[3]Department of Civil, Environmental and Mechanical Engineering, Università di Trento, Trento, Italy
[4]Institute of Earth Surface Dynamics, Faculty of Geoscience and the Environment, Université de Lausanne, Lausanne, Switzerland
[5]Dipartimento di Ingegneria Civile, Edile e Ambientale, Università di Padova, Padova, Italy

Correspondence: Concetta D'Amato (concetta.damato@epfl.ch)

Abstract.

Ecohydrology is a rapidly evolving interdisciplinary field. It explores the interactions among the variety of hydrological processes and ecosystems, specifically water controls on the biota. Advances in measurement techniques and modeling frameworks have enhanced our understanding of key processes, such as vegetation-rainfall interactions, soil moisture dynamics, water-borne disease infections, and the impacts of landscape evolution on streamflow. However, most existing ecohydrological models rely on rigid, predefined components and parameterisations, which limit their flexibility to diverse case studies and datasets. Addressing these limitations requires the implementation of open-source modular frameworks that facilitate customization, comparison, and integration of several modeling components.

The present study introduces and validates GEOSPACE (Soil-Plant-Atmosphere Continuum Estimator), a flexible, open-source ecohydrological framework within the GEOframe system. GEOSPACE employs object-oriented programming principles to model mass and energy fluxes within the critical zone, focusing on processes such as evapotranspiration, soil water dynamics, and vegetation water uptake. Its modular architecture offers multiple alternative formulations for key processes, allowing researchers to tailor simulations to specific scenarios, compare different models, and extend the capabilities of the model. The study uses data from a previous experiment to demonstrate the effectiveness of GEOSPACE in simulating ecohydrological processes under diverse conditions. GEOSPACE is therefore identified as a valuable tool for addressing critical ecohydrological challenges, paving the way for innovative and reliable solutions in a changing environmental context.

1 Introduction

Rodriguez-Iturbe (2000) defined ecohydrology as "the hydrologic mechanisms underlying the climate-soil-vegetation dynamics and thus controlling the most basic ecological patterns and processes". Ecohydrology is an interdisciplinary field that

https://doi.org/10.5194/egusphere-2026-2385
Preprint. Discussion started: 28 July 2026

analyses the interactions between hydrological processes and ecological systems to address how water availability and dynamics control the distribution, structure, and functioning of life across scales, from the soil-plant-atmosphere continuum (SPAC) within the Earth's Critical Zone (CZ) to entire catchments (Porporato and Yin, 2022; Rinaldo and Rodriguez-Iturbe, 2022; Rinaldo, 2024). Traditionally focused on the critical zone as the domain where climate, soil, and vegetation interact, ecohydrology now encompasses broader hydrologic controls on biota, recognizing river basins as fundamental ecological and hydrological control volumes that link geomorphology, biodiversity, and ecosystem sustainability (Rinaldo and Rodriguez-Iturbe, 2022).

Over the past two decades, the field of ecohydrology has experienced substantial progress, highlighted by the establishment of a dedicated journal in 2008 (Smettem, 2008) and the growing integration of advanced remote sensing technologies and modeling frameworks. These developments have greatly improved our ability to investigate the complex interactions among vegetation and soil moisture dynamics (Grant and Dietrich, 2017; Guswa et al., 2020). As discussed by Guswa et al. (2020) some key ecological questions raised, including how vegetation canopies interact with rainfall to influence water fluxes, how critical zone processes distribute soil moisture between transpiration and groundwater, and how landscape changes impact streamflow quantity, distribution, and quality. The challenges of the 21st century, particularly in relation to water for agriculture, require the development of tools to optimise irrigation and manage resources in the context of climate change, population growth, and availability of water resources (Guswa et al., 2020; Smith et al., 2024). Integration of ecological and hydrological processes is imperative to address the impacts of climate change and anthropogenic activities on water quality and quantity (Cao et al., 2022).

Addressing ecohydrological challenges requires the use of flexible modeling frameworks capable of being effectively integrated with observational data. A model can be considered as a selection of processes and equations deemed representative of the key processes under investigation. However, it is clear that a given process can be represented by multiple equations. For example, evaporation and transpiration can be modeled through simplified temperature-based approaches like Hargreaves (Hargreaves, 1989), radiation-based approaches like Priestley-Taylor (Priestley and Taylor, 1972) which only requires net radiation and temperature, to more physically-based formulations like Penman-Monteith (Penman and Keen, 1948) which accounts for aerodynamic and surface resistance, up to more complex methods that explicitly solve the canopy energy balance and leaf temperature, accounting for leaf area index and the partitioning of radiation between sunlit and shaded canopy layers (D'Amato and Rigon, 2025). Other classic examples involve modeling of soil water fluxes, where efforts to include the effects of soil structure have led to the adoption of advanced retention curves beyond Van Genuchten's parameterization (Tubini and Rigon, 2022).

Many ecohydrological models have been developed to simulate the coupled dynamics of water, energy, and vegetation within the SPAC, spanning a wide spectrum of complexity and process representation. Conceptual models represent water storage through lumped reservoirs with simplified flux parameterisations, while physically-based frameworks are grounded in first principles, from the Richards equation for unsaturated soil water flow to biochemical models of stomatal conductance and carbon assimilation. Among the latter, HYDRUS (Simunek et al., 2005) focuses on water and solute transport in the vadose zone; Tethys-Chloris (T&C) (Fatichi et al., 2012) couples vegetation carbon dynamics with a full soil-plant-atmosphere water and energy balance; EcH2O-iso (Kuppel et al., 2018) integrates the tracking of stable water isotopes and water age to

https://doi.org/10.5194/egusphere-2026-2385
Preprint. Discussion started: 28 July 2026

constrain hydrological fluxes. Despite this diversity, a common limitation of existing models is the use of a fixed set of process representations and constitutive equations, which leaves users with limited scope to modify the model structure or replace individual process formulations. This rigidity makes it difficult to isolate the contribution of individual components to the overall model response and to adapt the framework to different scientific questions or environmental contexts. Consequently, there is a growing need for modeling platforms that enable the flexible selection, integration, and intercomparison of process representations. In an era where research transparency and reproducibility have become fundamental requirements of the scientific community, such platforms should furthermore be open-source, ensuring that model assumptions, equations, and results remain fully accessible and verifiable.

In this regard, the GEOframe system and its Soil-Plant-Atmosphere Continuum Estimator (GEOSPACE) (D'Amato et al., 2025a) stand out as a pioneering approach. GEOframe is an open-source, component-based hydrological modeling system (Formetta et al., 2014; Bancheri et al., 2020), where each part of the hydrological cycle is implemented in a self-contained building block, an OMS3 component (David et al., 2013), covering processes ranging from geomorphic analysis and spatial interpolation of meteorological variables to evapotranspiration, runoff generation, and model calibration. GEOSPACE is the ecohydrological core of GEOframe, designed to simulate interactions within the SPAC and analyze processes occurring in the Critical Zone (National Research Council et al., 2001). It models the mass and energy budgets as well as water flow along a soil profile, accounting for water uptake by vegetation as transpiration flux. GEOSPACE is built on object-oriented programming (OOP), which provides the architectural foundation for its modular and extensible design. Having a truly modular structure goes beyond simply offering multiple options within a fixed model architecture. In a modular framework, individual components can be added, removed, or replaced independently, without requiring modifications to the rest of the code. GEOSPACE offers multiple alternatives for the same physical processes, varying in complexity and level of detail, which enables users to tailor model components to their specific case study, compare alternative modeling approaches under identical boundary conditions, and incorporate new features to enhance the robustness and reliability of their simulations. The component-based structure is furthermore designed to improve software robustness and facilitate testing and inspection by third parties, and the software adheres to modern software engineering practices (Rigon et al., 2022) and FAIR principles (Findable, Accessible, Interoperable, and Reusable) (Wilkinson et al., 2016). However, the effectiveness of GEOSPACE's modularity and its capability to investigate real-world ecohydrological systems has not been tested yet.

In this study, we build on data from a previously published controlled experiments in large lysimeters to demonstrate the potential of the GEOSPACE framework in addressing ecohydrological challenges. Our objectives are to i) validate GEOSPACE by showcasing a selection of components that effectively simulate real-world ecohydrological data, ii) highlight the capabilities and advantages of its modular structure, iii) demonstrate that GEOSPACE enables novel ecohydrological analyses that pave the way for addressing future scientific and environmental challenges.

https://doi.org/10.5194/egusphere-2026-2385
Preprint. Discussion started: 28 July 2026

2 Material and Methods

2.1 GEOSPACE modeling framework

Integrated into the GEOframe system, GEOSPACE (D'Amato et al., 2025a) is specifically designed to simulate the interactions within the SPAC system across the Earth's Critical Zone. It comprises three core components: WHETGEO, which handles water, heat, and solute transport (Tubini, 2021; Tubini and Rigon, 2022); GEOET, dedicated to evapotranspiration modeling and BrokerGEO, which acts as a coupler between these modules (D'Amato, 2024). Each component serves a distinct and complementary role, with a focus on modularity and extensibility. WHETGEO employs the Newton-Casulli-Zanolli algorithm (Casulli and Zanolli, 2010) to solve the Richards-Richardson equation, enabling robust simulations of soil water dynamics. GEOET provides a suite of evapotranspiration models (e.g., GEOET-Prospero, GEOET–Priestley–Taylor) (D'Amato et al., 2025a), allowing users to select the most appropriate formulation for their specific study. BrokerGEO facilitates seamless data exchange between components in memory, ensuring efficient partitioning of evapotranspiration fluxes into soil control volumes taking into account the actual root density distribution. This integrated and modular design improves the flexibility and functionality of GEOSPACE (D'Amato et al., 2025a).

2.2 Data description of "Spike II" experiment

The validation of the GEOSPACE framework is centered around data from the "Spike II" experiment (Benettin et al., 2021a), in which 4 soil columns planted with different vegetation types were monitored over a two-months period. The experiment was conducted in 2018 on the EPFL campus in Lausanne, Switzerland.

Each soil column (also referred to as 'weighed lysimeter' or simply 'lysimeter') consists of a fiberglass vessel measuring 2.5 meters in depth and encompassing a surface area of 1.12 m^2 (Figure 1). The vessels rest on load cells that measure weight continuously and allow for accurate estimations of total evapotranspiration (Benettin et al., 2021a; Peters et al., 2017). All lysimeters were filled 3–6 years before the experiment with a combination of sandy soil, comprising approximately 50% loamy sand from a nearby construction site and 50% lacustrine sand from Lake Geneva. The lysimeter with the willow tree (L2 in Figure 1) was filled with this soil mixture to a depth of 2 meters and it was the most instrumented. Its drainage system consisted of a 50-cm gravel filter below the soil, with a syphon at 225 cm depth to maintain a realistic pressure profile within the soil (Figure 1). Flow out of the syphon was measured through a tipping bucket. Inside the column, volumetric water content, temperature and soil water potential were measured at depths of 25 cm, 75 cm, 125 cm and 175 cm (2 FDR probes and 1 tensiometer per depth). The tree had a height of approximately 3.5 m, although branches were progressively removed for xylem and leaf water sampling throughout the experiment (Nehemy et al., 2021; Benettin et al., 2021a). The rooting system reached down to 2-m depth, where a geotextile prevented roots from going deeper into the gravel filter. The rooting system had relatively high and uniform fine root length density (RLD) and root tissue density (RTD), with RLD ranging between 14.24 cm cm^{-3} (top layer) and 6.47 cm cm^{-3} (bottom layer) (see Nehemy et al., 2021). The other three lysimeters were made shorter by the use of a permeable barrier at 1-m depth, which also guaranteed free drainage conditions at the bottom (no syphon). These lysimeters did not have sensors installed within the soil nor a bottom flow gauging system, but their evapotranspiration

https://doi.org/10.5194/egusphere-2026-2385
Preprint. Discussion started: 28 July 2026

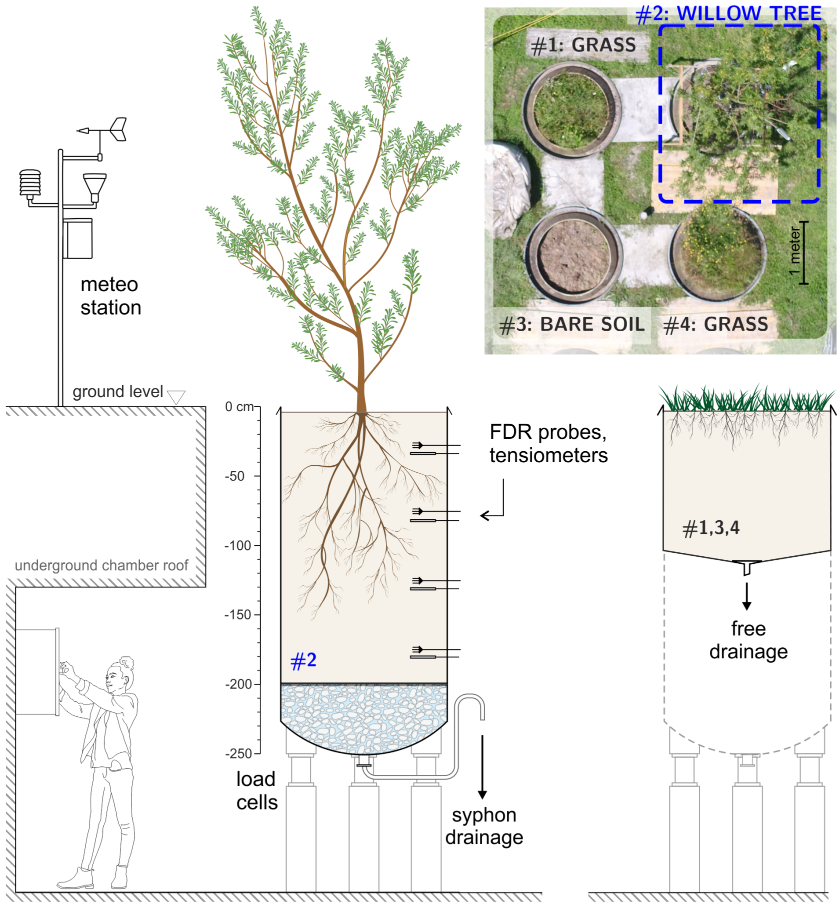

Figure 1. Sketch of the experimental setup of the "Spike II" experiment (Benettin et al., 2021a), highlighting the different soil depths and vegetation covers across the different columns.

could be estimated from the recorded weight variations. These lysimeters had different soil cover: lysimeter 3 (L3) was kept bare soil, while lysimeters 1 and 4 (L1 and L4) were vegetated with spontaneous grass in the 2 years prior to the experiment. The atmospheric conditions (2) were monitored through a meteorologic station installed 5 meters away from the lysimeters. Occasional documented amounts of irrigation water were provided to the lysimeter with the willow tree. Further insight into these datasets, including tree water deficit measurements and tracer data from a pulse tracer experiment are available from previous publications (Benettin et al., 2021a; Nehemy et al., 2021; Benettin et al., 2021b).

2.3 Model simulations setting

To conduct the simulations of the "Spike II" experiment and thus validate the GEOSPACE framework in the four different lysimeters, we configured the GEOSPACE model to faithfully reflect the environmental conditions and specific structure of the lysimeters during the experiment.

https://doi.org/10.5194/egusphere-2026-2385
Preprint. Discussion started: 28 July 2026

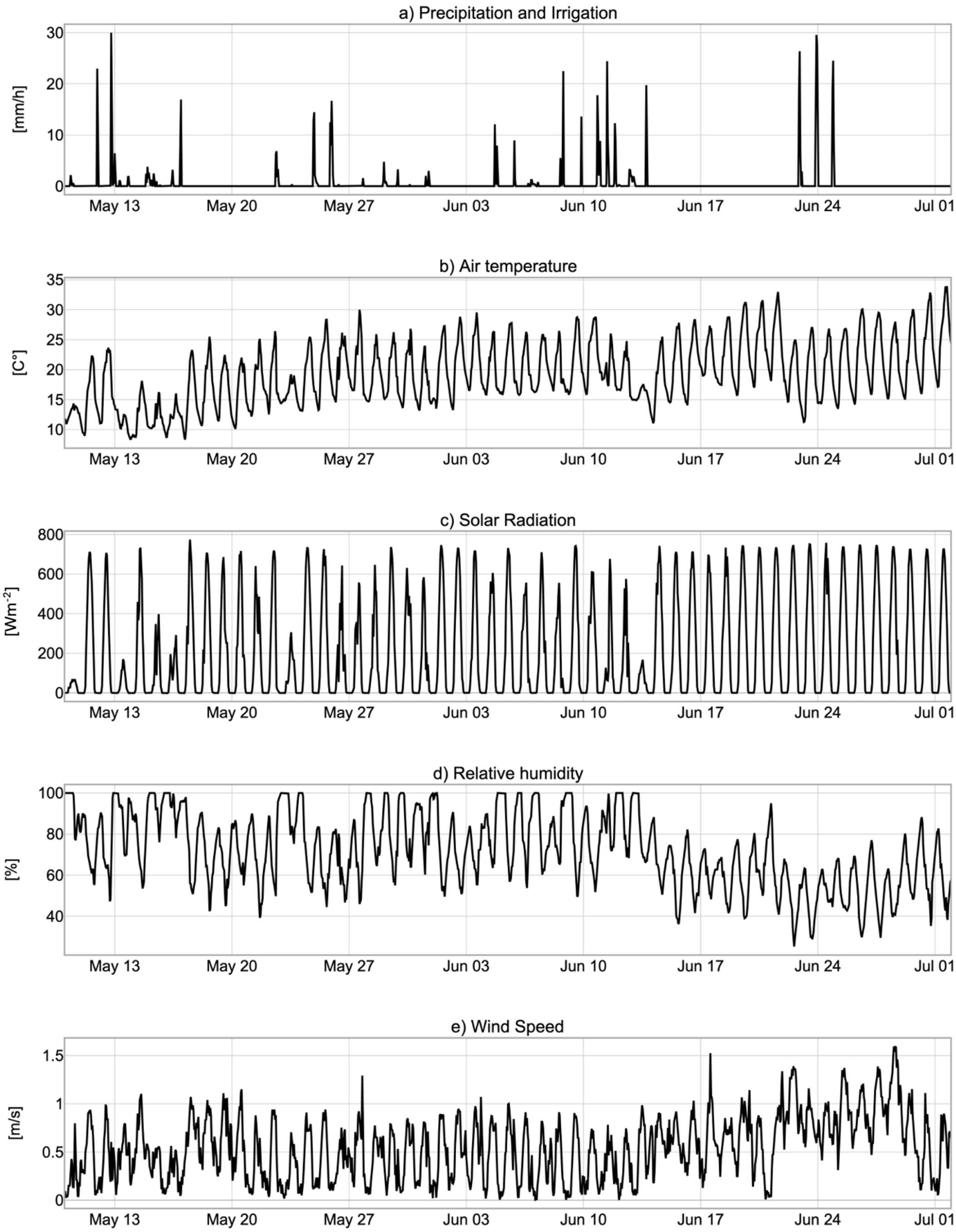

Figure 2. Hourly series of meteorologic data from the "Spike II" experiment (Benettin et al., 2021a).

https://doi.org/10.5194/egusphere-2026-2385
Preprint. Discussion started: 28 July 2026

Starting from the willow lysimeter (L2), the 2-meter homogeneous soil column was discretized into 100 control volumes. The drainage system, for modelling purposes, was represented as a layer of 20 control volumes, with the syphon implemented through a 'Seepage' bottom boundary condition, which triggers drainage when the hydraulic conductivity of the last control volume equals the saturated hydraulic conductivity. Thus, the total discretized depth of 2.25 m corresponds to the overflow height of the syphon.

The time step of the simulation is hourly with a model accuracy of two picard iterations per time step. Soil hydraulic properties are described with the Van Genuchten's model (Table 1). For the soil, the saturated water content θ_s, residual water content θ_r, saturated hydraulic conductivity K_s, and empirical parameters α and n were taken from Asadollahi et al. (2022), while water content at wilting point θ_{WP} and field capacity θ_{FC}, were calibrated manually. For the saturated gravel filter below the syphon level, all parameters were set equal to those of the soil, except for the saturated hydraulic conductivity K_s, which was calibrated independently.

Table 1. Hydraulic properties used to simulate the soil column with the willow tree (L2) .

Depth [m]	θ_r [-]	θ_s [-]	θ_{WP} [-]	θ_{FC} [-]	α [m^{-1}]	n [-]	K_s [$\mathrm{m\,s}^{-1}$]
0 - 2	0.05	0.3	0.0803	0.205	6	1.31	3.47×10^{-5}
2 - 2.25	0.05	0.3	0.0803	0.205	6	1.31	1.38×10^{-7}

The data input for the model came from the meteorologic station. The top boundary condition of the simulation was prescribed as "Top Coupled", with rainfall and irrigation as input timeseries. In WHETGEO, the soil surface is represented by an additional computational node coupled with the shallow water equations (Tubini and Rigon, 2022). This node tracks the ponding water depth $H(\psi)$, which is positive when water accumulates at the surface and zero otherwise. Thanks to this formulation, the surface boundary condition automatically transitions between a Neumann type (prescribed flux) and a Dirichlet type (prescribed water suction), without requiring any explicit switching technique, a numerical advantage that ensures stability across the full range of surface conditions, from dry infiltration to surface ponding. The initial water pressure within the soil column was derived from the measured water content values at the beginning of the simulation, by inverting the soil water retention curve (SWRC) and deriving the corresponding ψ values.

For the evapotranspiration model, we used the GEOET-ProsperoPM model, which combines GEOET-Prospero for transpiration and GEOET-Penman-Monteith for evaporation. The model input data (Figure 2) came from the meteorologic station. We used the total measured solar radiation to compute transpiration, but only the fraction of radiation hitting the soil to compute evaporation from soil. The latter radiation is calculated through the Sun/Shade model introduced by (de Pury and Farquhar, 1997) as described in D'Amato (2024) and D'Amato et al. (2025a). The height of the willow was fixed to 3.5 m (Benettin et al., 2021a). Since the willow leaf area index (LAI) is a key parameter for the evapotranspiration component but it was not measured, we estimated this variable based on literature values (Merilo et al., 2006; Heinsoo et al., 2004) considering a 6-year-old willow tree. Accordingly, LAI was prescribed to range between 6 and 6.5 until June 21st, after which the plant was

https://doi.org/10.5194/egusphere-2026-2385
Preprint. Discussion started: 28 July 2026

partially harvested. From that date onward, LAI was fixed at 4 for the remainder of the simulation. Furthermore, we adopted the measured root depth and root density parameters.

GEOET implements multiple stomatal conductance models (D'Amato et al., 2025a); here we adopted the Jarvis model (Jarvis et al., 1976), in which the stomatal conductance depends on multiplicative stress functions for radiation, temperature, vapour pressure deficit, and soil water availability (White et al., 1999; Macfarlane et al., 2004). Among these, we focused on the soil water stress component and expressed it as a linear stress factor $g_{w,i} \in [0,1]$ based on the fraction of transpirable soil water (Sinclair and Ludlow, 1986). The soil water stress function was implemented following D'Amato et al. (2025a) and defined for each control volume i as:

$$g_{w,i} = \frac{\theta_i - \theta_{WP,i}}{\theta_{FC,i} - \theta_{WP,i}} \tag{1}$$

where θ_i is the soil water content, and $\theta_{WP,i}$ and $\theta_{FC,i}$ are the wilting point and field capacity of the i-th control volume, respectively. Since transpiration is computed as a single plant-level flux, GEOET requires a single representative stress factor G_w rather than layer-specific values. Given that WHETGEO discretises the soil into multiple control volumes, each characterised by a local stress $g_{w,i}$, G_w must be derived by aggregating these local values across the root zone. For transpiration, G_{Tw} was computed as the root-density-weighted average:

$$G_{Tw} = \frac{\sum_{i=1}^{N} g_{w,i} \cdot \rho_{R,i}}{\sum_{i=1}^{N} \rho_{R,i}} \tag{2}$$

where $\rho_{R,i}$ is the root density in the i-th control volume and N is the number of control volumes intersected by the root system. For evaporation, the representative stress factor G_{Ew} was taken as the arithmetic mean of $g_{w,i}$ over the control volumes within the evaporation layer (0–0.2 m from the soil surface). The partitioning of E and T fluxes among control volumes is performed by BrokerGEO, following the same weighting by root density and local water stress. For additional details and numerical explanations of GEOSPACE, please refer to D'Amato et al. (2025a).

Table 2. Column discretization specifying for the two grass lysimeter (L1, L4) and the bare soil (L3) the respective depth, number of control volumes (CV) and soil type.

Lysimeter	Depth [m]	n° CV	ID Soil Type
L1	0 - 1.0	100	3
L4	0 - 0.5	60	4
L3	0 - 1.0	100	5

Regarding the grass and bare soil lysimeters, individual computation grids were constructed, each adapted to their experimental setup. These lysimeters featured a single-layer homogeneous soil column (see Table 2). The soil hydraulic parameters were initially transferred from the willow lysimeter setup and subsequently calibrated manually for each lysimeter. The resulting parameter values are detailed in Table 3, where differences from the willow configuration reflect both the distinct soil and vegetation characteristics of each lysimeter. Due to the absence of water content and pressure data for these lysimeters, the initial water pressure conditions of the soil columns were set as those of the willow lysimeter.

https://doi.org/10.5194/egusphere-2026-2385
Preprint. Discussion started: 28 July 2026

The simulations used as input the "Spike II" experimental meteorological dataset, without irrigation as these lysimeters were not irrigated. Details of all modeling configurations are outlined in Table 4. Notably, L1 and L4 exhibit distinct characteristics, with L4 featuring thicker and taller grass compared to L1; accordingly, different values for canopy height and leaf area index were assigned to the two lysimeters. Both were simulated using the GEOET-ProsperoPM formulation, combining GEOET-Prospero for transpiration and GEOET-Penman-Monteith for evaporation. For L3, no vegetation parameters were prescribed and transpiration was set to zero; evaporation was computed using GEOET-Penman-Monteith applied directly to the soil surface.

Table 3. Hydraulic properties of the soil column for the soil types of lysimeters L1, L3 and L4.

Lysimeter ID - Soil Type	θ_r [-]	θ_s [-]	θ_{WP} [-]	θ_{FC} [-]	α [m^{-1}]	n [-]	K_s [m s^{-1}]
L1 - 3	0.02	0.3	0.0303	0.225	6	1.31	3.47×10^{-5}
L4 - 4	0.02	0.3	0.0303	0.205	6	1.31	3.47×10^{-5}
L3 - 5	0.05	0.3	0.0803	0.289	6	1.31	3.47×10^{-4}

Table 4. Summary of the main settings for simulations of the lysimeters with grass (L1, L4) and bare soil (L3).

<table>
<tr><th></th><th>L1</th><th>L4</th><th>L3</th></tr>
<tr><td>Time step simulation</td><td colspan="3">Hourly</td></tr>
<tr><td>Top boundary condition</td><td colspan="3">Top Coupled</td></tr>
<tr><td>Bottom boundary condition</td><td colspan="3">Free drainage</td></tr>
<tr><td>Canopy height</td><td>0.20 m</td><td>0.35 m</td><td>-</td></tr>
<tr><td>LAI</td><td>1.5 - 4</td><td>2.5 - 4.5</td><td>-</td></tr>
<tr><td>Root depth</td><td>0.25 m</td><td>0.30 m</td><td>-</td></tr>
<tr><td>Evaporation depth</td><td colspan="3">0.20 m</td></tr>
<tr><td>Type of stress applied</td><td colspan="3">Water stress</td></tr>
<tr><td>G^n_{Tw}</td><td colspan="2">RootDensityWeightedSF</td><td>-</td></tr>
<tr><td>G^n_{Ew}</td><td colspan="3">AverageSF</td></tr>
<tr><td>Transpiration splitter</td><td colspan="2">RootWaterWeightedMethod</td><td>-</td></tr>
<tr><td>Evaporation splitter</td><td colspan="3">AverageWaterWeightedMethod</td></tr>
</table>

3 Results

3.1 Model validation

Figure 3 illustrates the temporal and depth variations in water pressure within the willow lysimeter simulation and Figure 4 shows the time series of simulated transpiration and evaporation. Using GEOET-Prospero model, we estimate transpiration

https://doi.org/10.5194/egusphere-2026-2385
Preprint. Discussion started: 28 July 2026

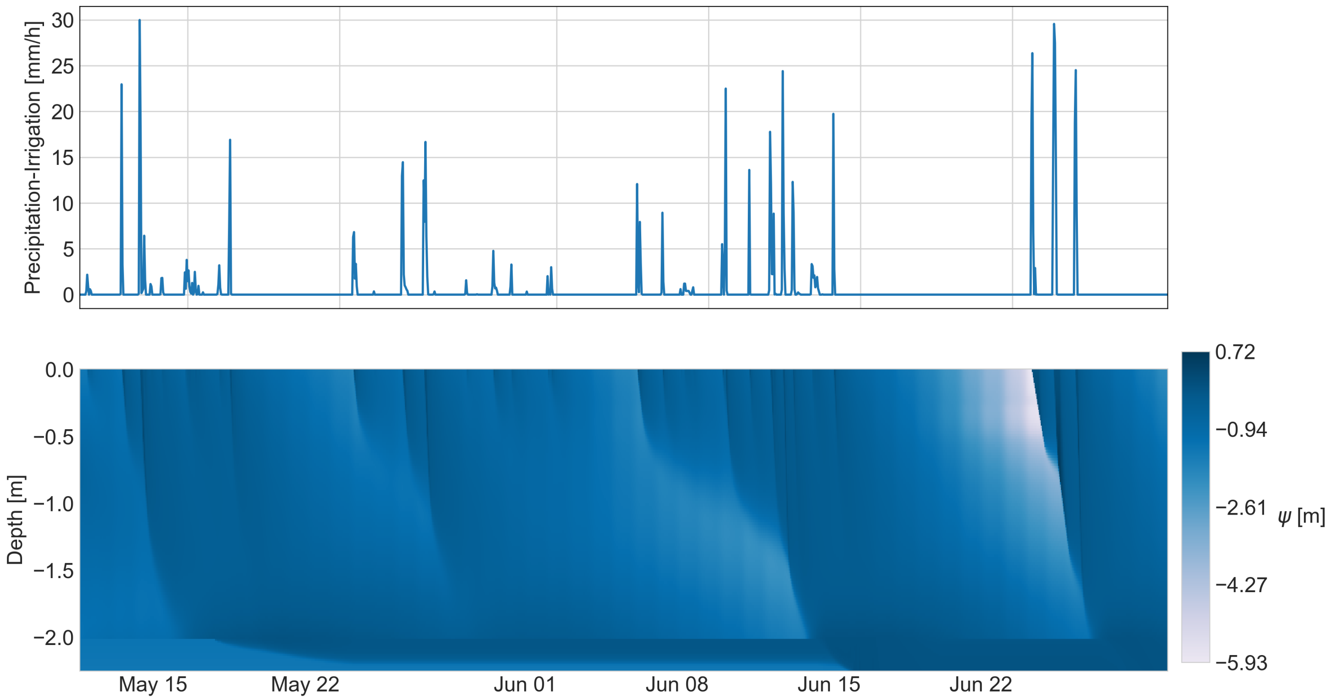

Figure 3. Precipitation-Irrigation and Soil Water Potential behavior in Willow tree simulation. The upper plot depicts precipitation-irrigation in millimeters per hour over time. The lower plot displays depth in meters, with a color scale representing soil water potential (ψ) along the depth.

(T) and evaporation (E) separately. In our analysis, the hourly ratio between evaporation and evapotranspiration (E/ET) ranged from 1% to 10%, with a daily average of 2%, which is consistent with the expected range. As reported by Benettin et al. (2021a), experimental observations indicate E/ET ratios between 5% and 10%. Such relatively low evaporation values are reasonable given the plant species, as the measured transpiration was very high, reaching daily maxima of up to 20 mm, in agreement with Frédette et al. (2019).

Leveraging the extensive dataset obtained from the lysimeter experiment, we conduct a comparative analysis of simulated water content against measured data at four distinct depths. Specifically, Figure 5 presents the normalized water content observed and simulated at depths of 0.25 m, 0.75 m, 1.25 m, and 1.75 m. Notably, Panel e) of the figure depicts the comparison concerning the bottom drainage.

The evapotranspiration flux derived from the willow lysimeter simulation (Figure 4) was compared with data obtained from weight measurements of the L2 lysimeter. Figure 6 presents this comparison in Panel a). Panel b) provides an in-depth analysis of the evapotranspiration distributions. Furthermore, the residual error of the model, calculated as the difference between simulation and measurements, is depicted in Panel c). Analyzing its distribution we obtained a mean residual error of 0.01 mm/h.

https://doi.org/10.5194/egusphere-2026-2385
Preprint. Discussion started: 28 July 2026

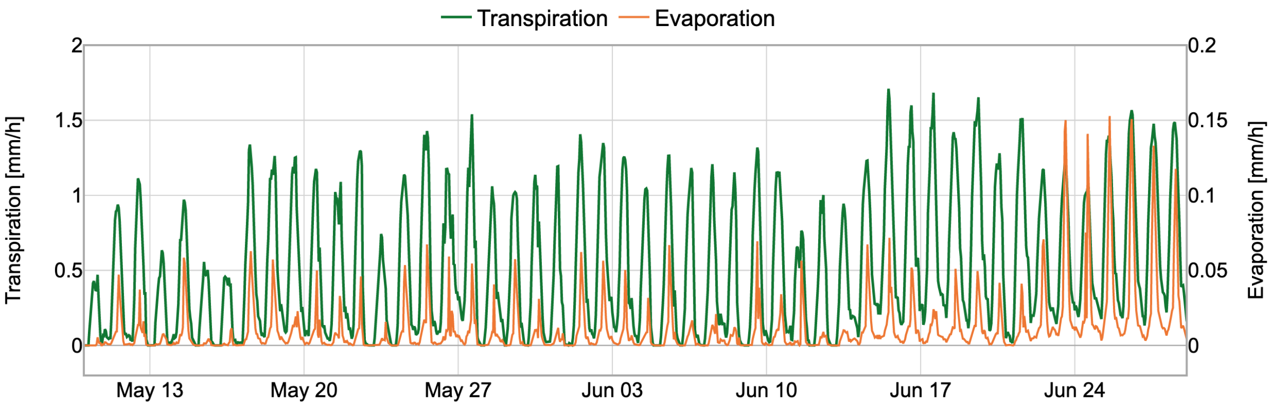

Figure 4. Time series of simulated transpiration (green) and evaporation (orange) fluxes [mm h^{-1}]. Transpiration is plotted on the primary y-axis (left) and evaporation on the secondary y-axis (right).

Figure 7a represents the scatterplot of the simulated evapotranspiration values compared to the measured ones for the willow lysimeter simulation during daytime hours (6:00 - 20:00). Further details and additional data pertaining to this simulation can be found in the supplementary material Notebooks. The simulations featured a mean mass balance error of -1.29×10^{-8} m, indicating that the error remains insignificant across the entire simulation.

Concerning the grass and bare soil lysimeters, the experimental procedure involved only the weight measurement, from which the evapotranspiration flux for L1 and L3, and the evaporation flux for L4, were derived. Figures 7b, 7c and 7d show scatter plots that illustrate the comparison between the simulated and measured values, respectively, for the grass lysimeter L1, the grass lysimeter L4 and the bare soil lysimeter L3, along with their respective values of R^2. during daytime hours (6:00 - 20:00). A comprehensive analysis of the evapotranspiration fluxes is elaborated in detail in Supplemental Material. Further details and additional data pertaining to these simulations can be found in the dedicated folder available on the Zenodo repository (D'Amato et al., 2026).

A distinctive feature of GEOSPACE is its ability to simulate the temporal and vertical dynamics of root water uptake (RWU) across the entire soil column (D'Amato et al., 2025a). The model computes RWU in each control volume (CV) of the discretized soil profile, which enables the computation of the mean depth of water uptake (Figure 8). The figure illustrates how different portions of the soil profile contribute to daily transpiration. The upper panel shows the simulated daily transpiration flux, while the lower panel displays the relative contribution of each CV to total RWU, obtained by normalizing the RWU in each CV by the daily transpiration.

https://doi.org/10.5194/egusphere-2026-2385
Preprint. Discussion started: 28 July 2026

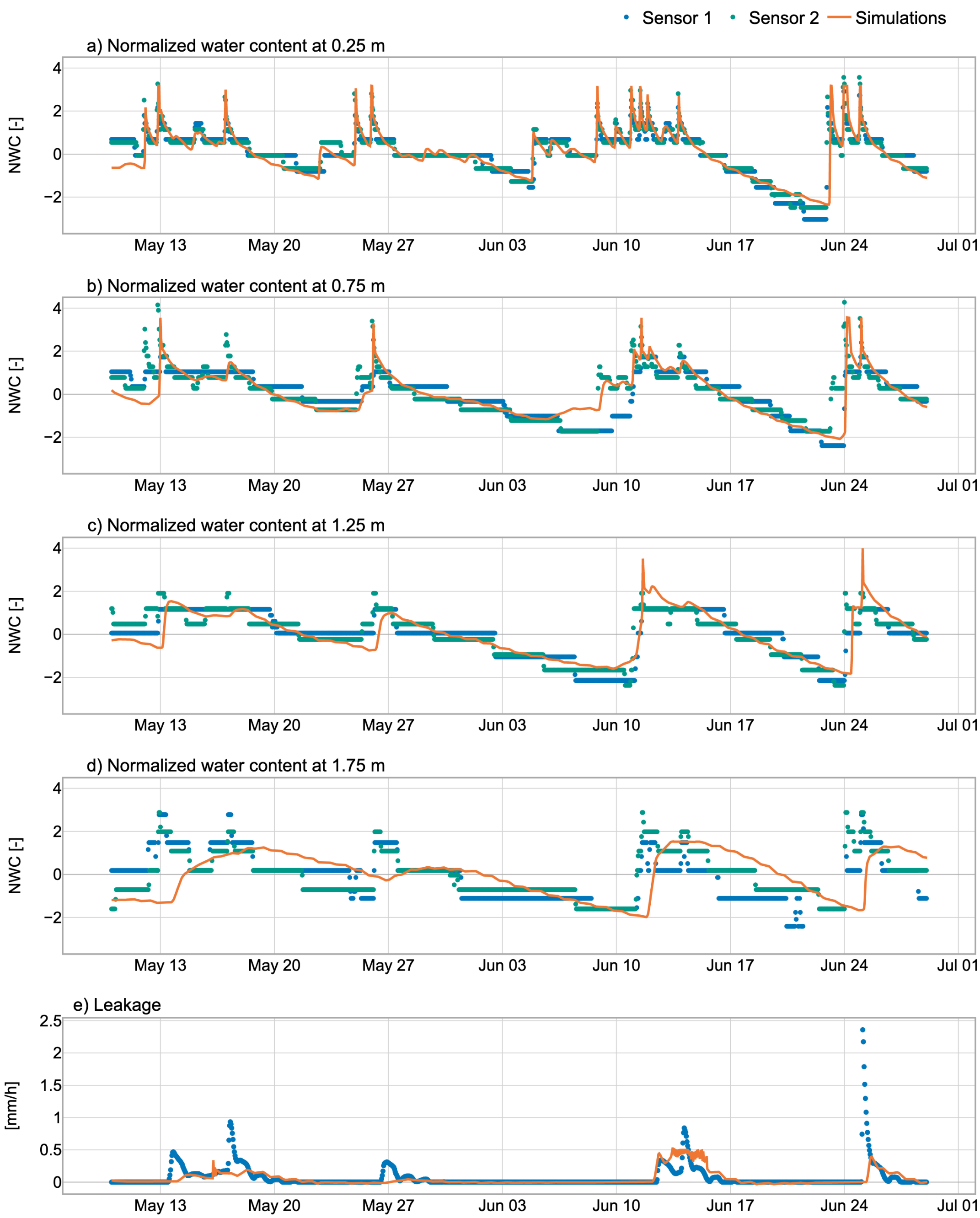

Figure 5. Comparison between experimental data (green and blue dots) and GEOSPACE simulations (orange line) for the willow lysimeter. Panels a) - f) show the comparison of normalized water content (NWC) for the four depths analyzed, Panel e) shows the comparison for the leakage at the bottom of the lysimeter.

https://doi.org/10.5194/egusphere-2026-2385
Preprint. Discussion started: 28 July 2026

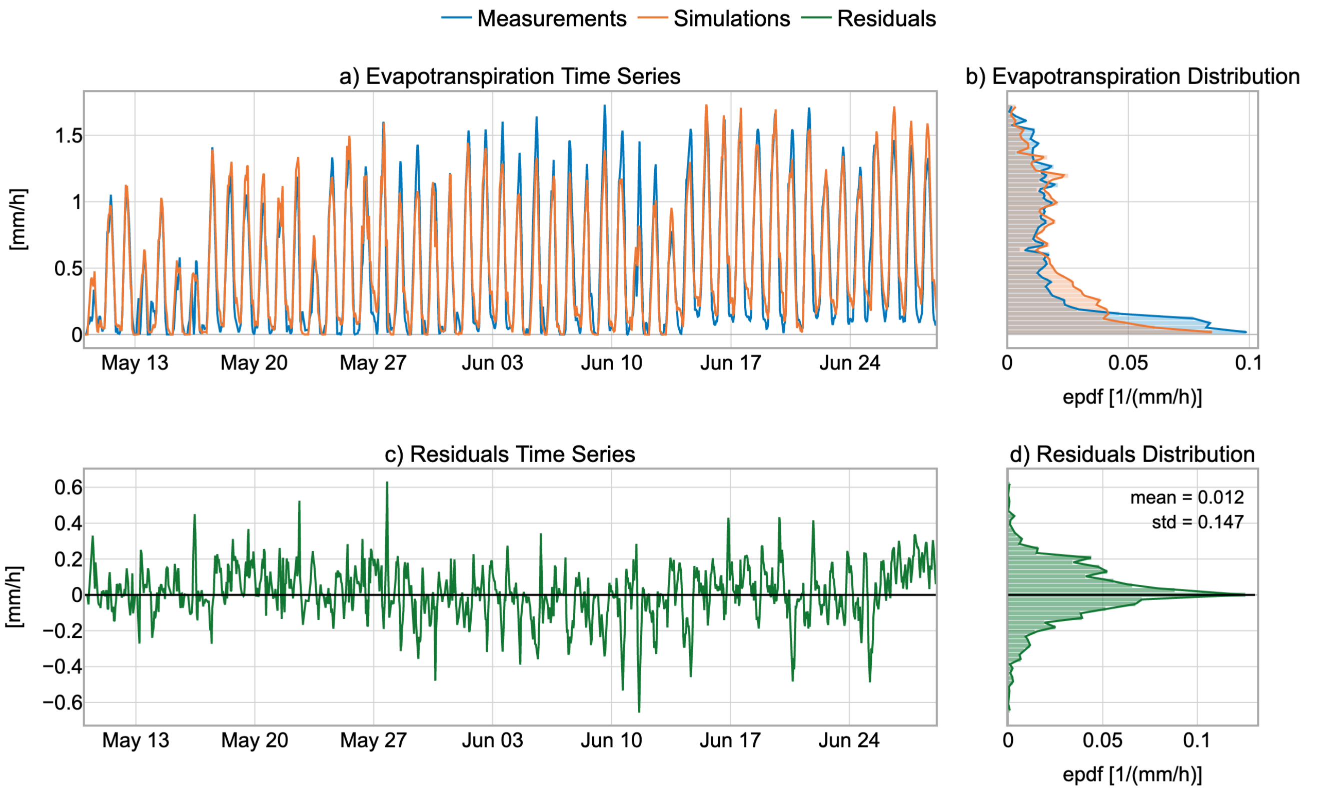

Figure 6. Analysis of evapotranspiration time series and distributions in the willow tree simulation. Panels a) and b) depict time series and distributions of evapotranspiration, while Panels c) and d) highlight residuals and their distributions.

3.2 Example of GEOSPACE modularity

Model validation against the willow lysimeter data in the "Spike II" experiment was performed using two specific modules within the GEOET framework (D'Amato et al., 2025a): GEOET-Prospero for transpiration and GEOET-Penman–Monteith for evaporation. This choice was motivated by the availability of detailed measurements for this experiment, which enabled the use of the most physically-based formulations provided in GEOET. To further assess the flexibility of GEOSPACE, we also simulated evapotranspiration with alternative GEOET formulations (D'Amato et al., 2025a): the GEOET–Priestley–Taylor (GEOET-PT) and GEOET–Penman–Monteith FAO (GEOET-PM-FAO) approaches (Figure 9). The soil component, represented by WHETGEO, was configured identically across all simulations to ensure that any differences in results arose solely from the choice of evapotranspiration formulation. Because the focus of this comparison is on the GEOET options within GEOSPACE, we report only the resulting evapotranspiration fluxes (Figure 9).

For the GEOET-PT model, measured radiation data (Figure 2) were used. No vegetation information was prescribed as this model does not require it. The coefficient α was calibrated to 4.16, starting from the standard value of 1.26 (Priestley and Taylor,

https://doi.org/10.5194/egusphere-2026-2385
Preprint. Discussion started: 28 July 2026

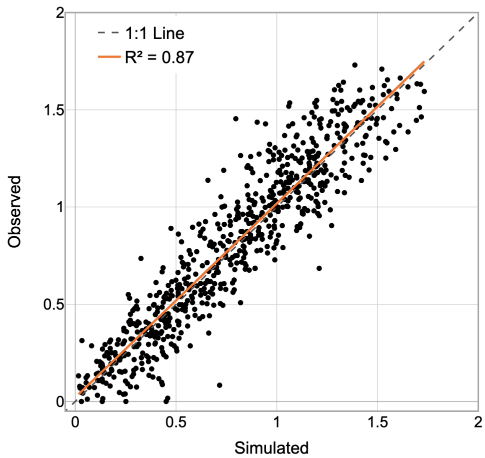

(a) Scatterplot for L2 willow lysimeter.

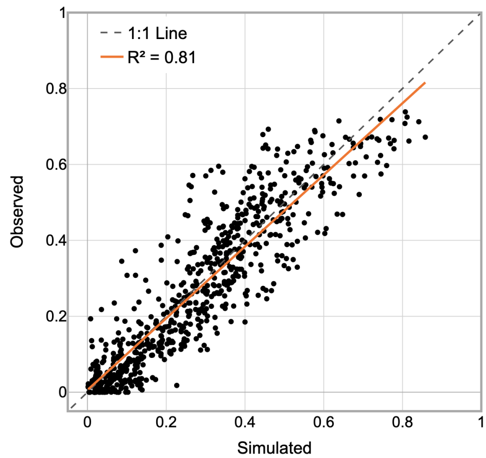

(b) Scatterplot for L1 grass lysimeter.

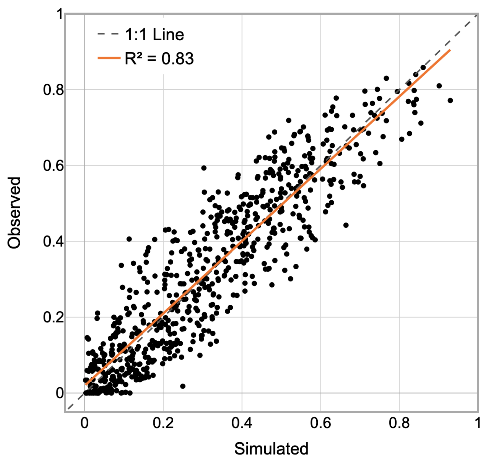

(c) Scatterplot for L4 grass lysimeter.

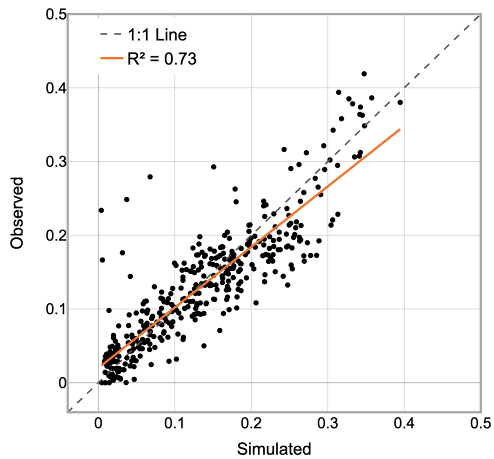

(d) Scatterplot for L3 bare soil lysimeter.

Figure 7. Comparison between experimental data and GEOSPACE simulation for the two grass lysimeters L1 and L4, and the bare soil L3 in daytime hour. Panel a) shows the scatterplot of evapotranspiration simulated versus observed values in Willow tree simulation during daytime. Panels b) and c) show the scatterplot of evapotranspiration simulated versus observed values respectively for L1 and L4. Panel d) shows the scatterplot of evaporation simulated versus observed values for L3. The dashed line indicates the perfect match while the orange one is the regression line with the specific R^2 value.

https://doi.org/10.5194/egusphere-2026-2385
Preprint. Discussion started: 28 July 2026

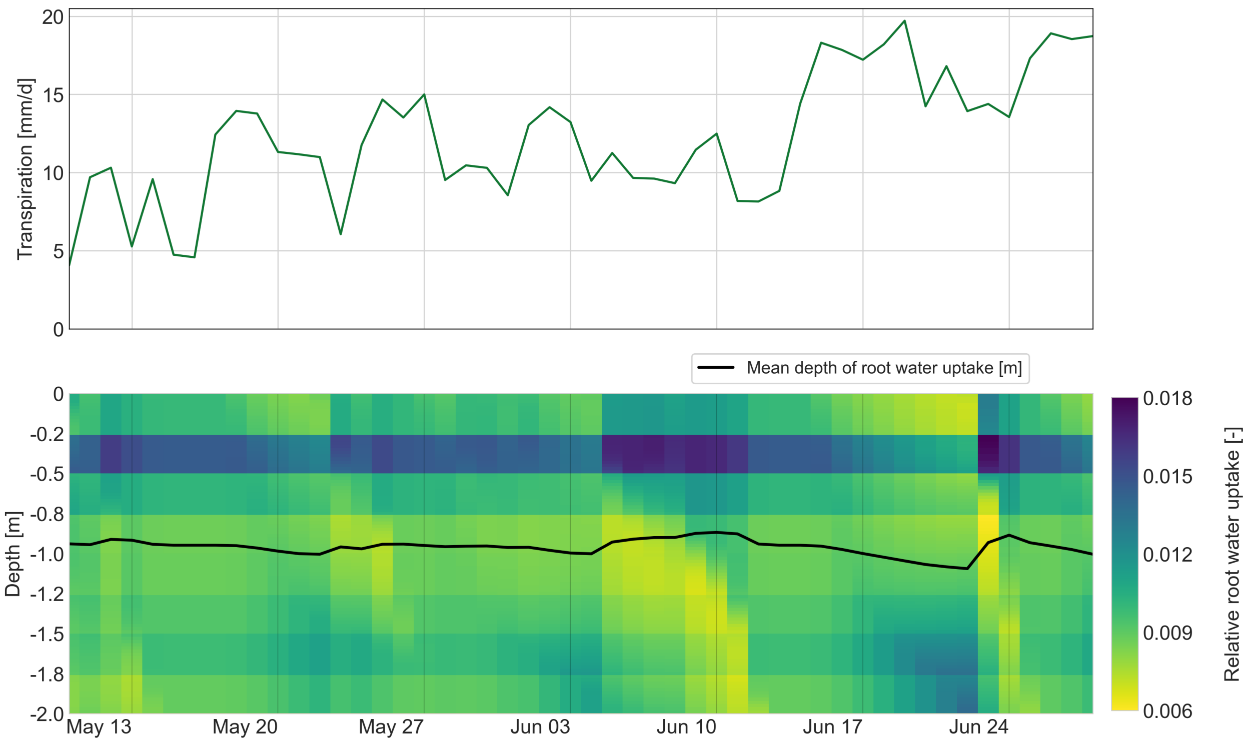

Figure 8. Temporal and spatial dynamics of root water uptake for the willow lysimeter. The upper panel shows the daily transpiration flux simulated with the GEOSPACE-Prospero-PM model. The lower panel represents soil depth [m] with a color scale indicating the relative root water uptake from each depth. The higher root water uptake (darker color) between 20 and 50 cm depth is due to the higher fine root density experimentally found at that depth. The black line depicts the temporal variation of the mean root water uptake depth.

1972). In the GEOET-PM-FAO simulation, both measured radiation and wind speed data from the meteorological station (Figure 2) were employed. Vegetation was prescribed through canopy height, root depth, and crop coefficient (K_c), with canopy height and root depth set to the same values used in the GEOET-Prospero-PM simulation (3.5 m and 2.0 m, respectively). K_c was calibrated to 3.9. Both simulations were carried out under water-stressed conditions only, with the representative stress factor G^{n}_{ETw} determined using the root density-weighted method (`RootDensityWeightedSF.java`), identical to the approach used in the validation simulation.

Figure 9 compares the hourly evapotranspiration simulated by GEOSPACE using the three GEOET formulations with the evapotranspiration derived from weight variations measured in the L2 lysimeter during the “Spike II” experiment. Because the strong diurnal cycle in the full time series makes visual comparison difficult, a 12-day zoom is shown to highlight the correspondence between simulations and measurements at the hourly scale. Daily and cumulative evapotranspiration show a similar ranking among the models; these time series and additional diagnostics are provided in the Supplementary Material.

https://doi.org/10.5194/egusphere-2026-2385
Preprint. Discussion started: 28 July 2026

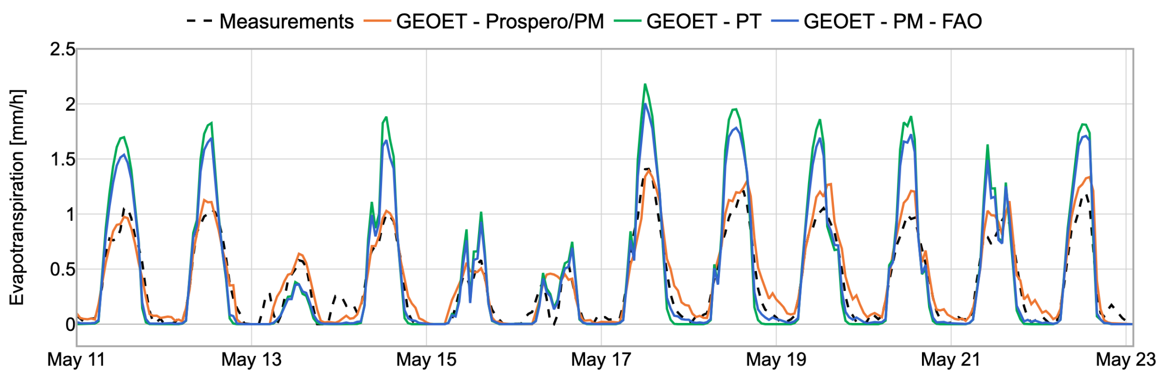

Figure 9. Twelve-day zoom of hourly evapotranspiration, comparing L2 lysimeter measurements from the "Spike II" experiment (black dashed line) with GEOSPACE simulations using three GEOET formulations: Prospero-PM (orange), Priestley–Taylor (green), and FAO Penman–Monteith (blue).

The mean residual error and standard deviation between simulated and measured hourly evapotranspiration for each GEOET formulation are shown in Table 5.

Table 5. Mean residual error and standard deviation between simulated and measured hourly evapotranspiration for the three GEOET formulations during the "Spike II" willow experiment. Residuals are computed as simulation minus measurements.

GEOET model	Prospero–PM	PT	PM–FAO
Mean residual [mm h^{-1}]	0.012	0.004	0.004
Standard deviation [mm h^{-1}]	0.147	0.296	0.247

4 Discussion

D'Amato et al. (2025a) presented the Soil-Plant-Atmosphere Continuum Estimator in GEOframe (GEOSPACE), a new ecohydrological modeling framework, and in particular its one-dimensional development, GEOSPACE-1D. In that work, the focus was on the model design principles, with an emphasis on modularity, extensibility, and numerical robustness. In this study, we advance that work by testing GEOSPACE against real experimental data and by demonstrating its practical applicability in different ecohydrological settings.

Our analysis was guided by three main research questions: i) Can GEOSPACE reproduce observed ecohydrological dynamics across contrasting vegetation and boundary conditions? ii) What are the capabilities and advantages of its modular structure? iii) Does GEOSPACE enable novel ecohydrological analyses that pave the way for addressing future scientific and environmental challenges? We discuss these questions in what follows.

https://doi.org/10.5194/egusphere-2026-2385
Preprint. Discussion started: 28 July 2026

4.1 Model behavior and performance across the “Spike II” lysimeters

The first objective of this work was to validate GEOSPACE by showcasing a selection of components that effectively simulate real-world ecohydrological data. We tested the model in four lysimeters from the “Spike II” experiment: a lysimeter with a willow tree (L2), two grass-covered lysimeters (L1 and L4), and a bare soil lysimeter (L3). These systems differ in vegetation structure, rooting depth, soil hydraulic configuration, and total column depth, and they were subject to both natural rainfall and controlled irrigation. Figures 3–7 show that GEOSPACE can realistically reproduce key hydrological and ecohydrological variables under these diverse conditions. In the willow lysimeter, the model reproduced the temporal evolution of soil water pressure along the vertical profile (Figure 3) and the partitioning between transpiration and soil evaporation (Figure 4). Simulated water content dynamics at four depths were in good agreement with FDR measurements (Figure 5), and the simulated drainage at the bottom of the column captured the main features of the observed leakage behavior, despite the complexity introduced by the siphon boundary condition. At the canopy scale, simulated evapotranspiration compared well with lysimeter-derived estimates (Figure 6). The residuals showed minimal bias (mean residual ≈ 0.01 mm h^{-1}), and the scatterplot between simulated and observed daytime fluxes yielded an R^2 of 0.87 (Figure 7a). GEOSPACE also produced consistent results for the other lysimeters. The three non-willow lysimeters differ from L2 not only in vegetation (grass or none versus a 3.5 m willow) but also in depth (shallower columns) and hydraulic properties. Despite these differences, simulated evapotranspiration fluxes agreed well with the values derived from weight variations for both grass lysimeters (L1 and L4, with $R^2 = 0.81$ and $R^2 = 0.83$, respectively) and for the bare-soil lysimeter (L3, $R^2 = 0.73$) (Figures 7b–d). The slightly lower performance over bare soil is likely related to the use of the Penman–Monteith formulation for evaporation, which does not account for soil thermal inertia; this omission can induce errors under conditions where heat storage and surface temperature dynamics significantly affect evaporation rates. The model’s ability to reproduce the behavior of all lysimeters within the same modeling framework suggests that GEOSPACE can be robustly parameterized across a broad range of conditions, from bare-soil evaporation to shallow-rooted herbaceous systems and deep-rooted woody vegetation. Taken together, these results indicate that GEOSPACE performs reliably as a process-based ecohydrological model under controlled and realistic environmental conditions. The model thus exhibits a combination of theoretical flexibility and practical applicability that supports its use under contrasting vegetation types, soil configurations, and boundary conditions.

4.2 Practical value of modularity

The second objective of this study was to illustrate the capabilities and advantages of GEOSPACE’s modular structure. Data availability remains a major limitation in ecohydrology: datasets such as “Spike II” are extremely valuable but rarely accessible, and most real-world applications must often rely on a smaller number of observed variables. GEOSPACE addresses this challenge through its modular design, which enables users to select among alternative mathematical representations of key processes. In the willow lysimeter, for example, evapotranspiration was simulated using three alternative formulations, GEOET–Prospero-PM, GEOET–Priestley–Taylor, and GEOET–Penman–Monteith FAO (Figure 9), while keeping the soil module (WHETGEO) and the evapotranspiration partitioning solver (BrokerGEO) identical across simulations. This configu-

https://doi.org/10.5194/egusphere-2026-2385
Preprint. Discussion started: 28 July 2026

ration isolates the effect of the evapotranspiration formulation itself, allowing a direct comparison among models of different physical complexity.

The choice of one formulation over another is not inherently "better" or "worse": all three approaches reproduced the total measured evapotranspiration over the full simulation period, in part because the calibration strategy enforced closure of the cumulative evapotranspiration mass balance (approximately 600 mm over the course of the experiment). Each formulation was calibrated using only one key parameter within the evapotranspiration module (LAI for Prospero-PM, α for Priestley–Taylor, and K_c for FAO Penman–Monteith). The calibrated values of α and K_c deserve explicit attention, as they reflect structural properties of the respective models rather than site-specific anomalies. The Priestley–Taylor coefficient α is not a universal constant: its value depends on the ratio of surface to aerodynamic resistance (Jarvis et al., 1976), and therefore increases with stomatal conductance and atmospheric coupling. For the willow lysimeter, where daily evapotranspiration peaks exceeded 20 mm d^{-1} and the tree maintained active stomatal control throughout the growing season, a calibrated value of 4.16, well above the standard 1.26, is physically expected: the Priestley–Taylor formulation, which contains no explicit representation of stomatal resistance, is forced to compensate through the single free parameter available to it. This behavior is consistent with the results of Bottazzi et al. (2021), who showed that Priestley–Taylor underperforms relative to Prospero-PM under conditions of high evaporative demand, precisely because it cannot resolve the stomatal regulation of transpiration. The same logic applies to $\mathrm{K}_c = 3.9$ in FAO Penman–Monteith: while this value falls within the upper range reported for willow in well-watered, highly productive conditions (Guidi et al., 2008; Frédette et al., 2019), it reflects the exceptionally high atmospheric demand of this specific system. In both cases, the out-of-range calibrated values are a diagnostic of the structural limitations of simplified formulations when applied to high-transpiration systems dominated by stomatal dynamics.

However, the way each model achieves the same cumulative flux differs markedly. As shown in Figure 9, the Prospero-PM formulation more accurately reproduces the sub-daily pattern, particularly the amplitude and timing of daytime peaks. This behavior is consistent with the lower standard deviation of the Prospero residuals, which is roughly half that of Priestley–Taylor and FAO Penman–Monteith, indicating improved agreement during periods of high evaporative demand. Capturing these peaks is not merely an aesthetic advantage: accurate sub-daily representations of evapotranspiration are essential for a correct estimation of the surface energy balance and leaf temperature, and become particularly critical under water-limiting conditions, where canopy processes are strongly controlled by short-term fluctuations in atmospheric demand. This improved performance is aligned with the physical basis of Prospero-PM. As shown in D'Amato et al. (2025a), the model solves the canopy-scale surface energy balance, providing latent and sensible heat fluxes as well as an explicit estimate of leaf temperature. Furthermore, its coupling with the Penman–Monteith formulation for soil evaporation separates soil and canopy contributions while accounting for the radiation reaching the soil surface based on a two-leaf sun–shade approach (de Pury and Farquhar, 1997). This level of detail improves the representation of vegetation–atmosphere interactions compared to the Priestley-Taylor or FAO Penman-Monteith models, and becomes increasingly relevant in light of growing interest in linking leaf temperature to stomatal regulation and isotopic fractionation within leaves (Cernusak et al., 2016).

One key advantage of this modular approach is that GEOSPACE allows users to employ physically explicit models when detailed inputs are available, or simpler parameterizations when they are not, without compromising the overall structure of

https://doi.org/10.5194/egusphere-2026-2385
Preprint. Discussion started: 28 July 2026

the simulation. While other ecohydrological models such as HYDRUS (Simunek et al., 2005), T&C (Fatichi et al., 2012), and EcH2O-iso (Kuppel et al., 2018) offer multiple process options within their respective frameworks, they are not designed around modularity as a core architectural principle. In GEOSPACE, components can be added, removed, or replaced independently without modifying the rest of the codebase (D'Amato et al., 2025a), meaning that users can implement entirely new process formulations and ensure they integrate seamlessly with the existing components, making GEOSPACE an extensible platform for ecohydrological research.

4.3 Further capabilities of GEOSPACE

GEOSPACE is well posed to address a number of ecohydrological problems beyond those demonstrated in the previous sections. As an example, we illustrate here how the distribution of root water uptake (RWU) simulated by the model (Figure 8) can directly link to a key problem in tracer-based ecohydrology.

A central question in ecohydrology is: how does vegetation make use of soil waters located at different depths and held at different water potentials (Sprenger et al., 2016; Dubbert and Werner, 2019; Freyberg et al., 2020)? Experimental approaches rely on water isotope measurements from the plant's xylem, which only provide a bulk measure of water uptake from the whole rooting system. Therefore, methods to resolve the uptake distribution over depth and relate it to physical mechanisms are needed.

GEOSPACE can help addresses this limitation by simulating RWU for each control volume and time step, yielding a full depth–time distribution of uptake intensity rather than a single representative value (Sprenger et al., 2016). In Figure 8, the temporal shifts in color patterns illustrate how the willow dynamically adjusts its water sources in response to soil moisture conditions and atmospheric demand: when the upper layer is drier (yellowish area), water uptake shifts to deeper layers. The black line, representing the mean RWU depth, provides a synthetic summary of this vertical shift over time. The spatial pattern of uptake closely mirrors the distribution of root density (Figure S1), confirming the strong structural control exerted by the root system architecture.

Several existing models, including HYDRUS (Simunek et al., 2005) and T&C (Fatichi et al., 2012), resolve RWU across individual soil layers. The distinctive contribution of GEOSPACE lies in integrating this depth-resolved uptake within a modular framework that couples root water sourcing directly with the surface energy balance and evapotranspiration partitioning. This capability is particularly relevant for identifying the portions of the root system sustaining transpiration during heatwaves, quantifying the buffering role of deep roots, and exploring vegetation feedbacks on vadose-zone storage. However, it should be noted that GEOSPACE does not currently include hydraulic redistribution. Incorporating this process could improve the representation of internal root water movement and refine RWU estimates under drought conditions. The modular design of GEOSPACE provides a clear pathway for such extensions: hydraulic redistribution can be added as an alternative process module without altering the existing soil or vegetation components.

Future developments will focus on refining stress representations, extending vegetation parameterizations, and applying GEOSPACE to a wide range of ecohydrological and environmental contexts. In particular, the model could be used to investigate how different root distributions affect soil water balance and plant resilience to drought, and to optimize irrigation strategies and water-use efficiency in agricultural systems under changing climatic and management conditions. Integrating advanced pedotransfer functions will improve soil hydraulic parameter estimation where data are limited, while the inclusion of leaf temperature dynamics will enable the coupling of thermal and isotopic analyses to better interpret plant water sourcing and stress responses. Beyond natural ecosystems, GEOSPACE can also be applied to quantify the cooling effects of urban vegetation and blue–green infrastructures, and to assess the impacts of climate change and extreme events, such as droughts, floods, and heatwaves, on the hydrological and ecohydrological feedbacks within the critical zone.

5 Conclusions

This study presents a comprehensive evaluation of the GEOSPACE model using experimental data from the "Spike II" lysimeter experiment, assessing its performance across four contrasting scenarios, a willow tree, two grass-covered lysimeters, and a bare soil system. The model successfully captured key hydrological dynamics such as infiltration, drainage, evapotranspiration, and root water uptake, showing strong agreement with experimental observations across diverse boundary and vegetation conditions.

These results confirm that GEOSPACE reliably represents coupled soil-plant-atmosphere processes across contrasting systems (research objective i). Beyond validation, our analysis further indicates that: (ii) its modular structure is scientifically useful, because it supports model intercomparison, transparency of assumptions, and graceful degradation under limited data availability; and (iii) it provides physically meaningful internal diagnostics, such as depth-resolved root water uptake, that help investigate not only "how much water is used" but also "where do plants extract water from". A direct comparison with isotopic tracer data would however require the integration of a transport model to simulate the movement of tracers through the soil and plant system.

Thanks to its open-source and component-based architecture (Rigon et al., 2022), and to its implementation following modern Object-Oriented Programming principles (Gamma et al., 1995), GEOSPACE is not just another ecohydrological model, but a flexible and extensible platform for process-based research. New process formulations can be integrated with minimal effort and without altering existing components. Its combination of physical consistency, transparency, and modularity makes it a reliable tool for investigating soil-plant-atmosphere interactions across a wide range of vegetation types, soil configurations, and boundary conditions.

Code and data availability. The source code of GEOSPACE, written in Java, is hosted on GitHub at https://github.com/geoframecomponents/GEOSPACE-1D and a frozen version at https://zenodo.org/records/16779108 (D'Amato et al., 2025c). Additionally, the corresponding OMS3 project is accessible at https://github.com/GEOframeOMSProjects/OMS_Project_GEOSPACE-1D and a frozen version is available on Zenodo at https://doi.org/10.5281/zenodo.16779840 (D'Amato et al., 2025b). Data used in this paper is available as part of the "Spike II" tracer experiment dataset (Nehemy et al., 2020), under Creative Commons Attribution (CC BY) license, at https://doi.org/10.5281/zenodo.4037240. The simulation presented in this work are available on the Zenodo repository at https://doi.org/10.5281/zenodo.19773215 (D'Amato et al., 2026).

https://doi.org/10.5194/egusphere-2026-2385
Preprint. Discussion started: 28 July 2026

Author contributions. C. D'Amato: Conceptualization, Methodology, Software, Validation, Investigation, Writing – Original Draft, Writing – Review & Editing, Visualization; P. Benettin: Conceptualization, Methodology, Validation, Supervision, Writing – Review & Editing; A. Rinaldo: Conceptualization, Supervision, Writing – Review & Editing; R. Rigon: Conceptualization, Methodology, Software, Supervision, Writing – Review & Editing

Competing interests. The authors declare no competing interests

Acknowledgements. This work has been supported by a Ph.D. grant by the Center Agriculture Food Environment - C3A at the University of Trento, by the Italian MIUR Project (PRIN 2017) "WATer mixing in the critical ZONe: observations and predictions under environmental changes-WATZON" (project code: 2017SL7ABC), and by COST Action WATSON (WATer isotopeS in the critical zONe from groundwater recharge to plant transpiration), CA19120 supported by COST (European Cooperation in Science and Technology), www.cost.eu. This study was partially carried out within the Space It Up project funded by the Italian Space Agency, ASI, and the Ministry of University and Research, MUR, under contract n. 2024-5-E.0 - CUP n. I53D24000060005.

References

Asadollahi, M., Nehemy, M. F., McDonnell, J. J., Rinaldo, A., and Benettin, P.: Toward a closure of catchment mass balance: Insight on the missing link from a vegetated lysimeter, Water Resour. Res., 58, 2022.

Bancheri, M., Rigon, R., and Manfreda, S.: The GEOframe-NewAge Modelling System Applied in a Data Scarce Environment, Water, 12, 86, 2020.

Benettin, P., Nehemy, M. F., Asadollahi, M., Pratt, D., Bensimon, M., McDonnell, J. J., and Rinaldo, A.: Tracing and closing the water balance in a vegetated lysimeter, Water Resour. Res., 57, 2021a.

Benettin, P., Nehemy, M. F., Cernusak, L. A., Kahmen, A., and McDonnell, J. J.: On the use of leaf water to determine plant water source A proof of concept, Hydrological Processes, 35, 2021b.

Bottazzi, M., Bancheri, M., Mobilia, M., Bertoldi, G., Longobardi, A., and Rigon, R.: Comparing evapotranspiration estimates from the GEOframe-Prospero model with Penman–Monteith and Priestley-Taylor approaches under different climate conditions, Water, 13, 1221, 2021.

Cao, Z., Wang, S., Luo, P., Xie, D., and Zhu, W.: Watershed ecohydrological processes in a changing environment: Opportunities and challenges, Water (Basel), 2022.

Casulli, V. and Zanolli, P.: A Nested Newton-Type Algorithm for Finite Volume Methods Solving Richards' Equation in Mixed Form, SIAM J. Sci. Comput., 32, 2255–2273, 2010.

Cernusak, L. A., Barbour, M. M., Arndt, S. K., Cheesman, A. W., English, N. B., Feild, T. S., Helliker, B. R., Holloway-Phillips, M. M., Holtum, J. A., Kahmen, A., McInerney, F. A., Munksgaard, N. C., Simonin, K. A., Song, X., Stuart-Williams, H., West, J. B., and Farquhar, G. D.: Stable isotopes in leaf water of terrestrial plants, Plant, Cell & Environment, 39, 1087–1102, https://doi.org/https://doi.org/10.1111/pce.12703, 2016.

D'Amato, C.: Exploring the Soil-Plant-Atmosphere Continuum: Advancements, Integrated Modeling and Ecohydrological Insights, Ph.D. thesis, Center Agriculture Food Environment (C3A), University of Trento, 2024.

D'Amato, C. and Rigon, R.: Elementary Mathematics Helps to Shed Light on the Transpiration Budget Under Water Stress, Ecohydrology, 18, e70 009, https://doi.org/10.1002/eco.70009, 2025.

D'Amato, C., Tubini, N., and Rigon, R.: A component-based modular treatment of the soil–plant–atmosphere continuum: the GEOSPACE framework (v.1.2.9), Geosci. Model Dev., 18, 7321–7355, https://doi.org/10.5194/gmd-18-7321-2025, 2025a.

D'Amato, C., Tubini, N., and Rigon, R.: OMS project for GEOSPACE-1D v.1.2.9, https://doi.org/10.5281/zenodo.16779840, 2025b.

D'Amato, C., Tubini, N., and Rigon, R.: GEOSPACE-1D v.1.2.9, https://doi.org/10.5281/zenodo.16779108, 2025c.

D'Amato, C., Benettin, P., Rinaldo, A., and Rigon, R.: Simulation data for: A flexible open-source modular framework for ecohydrological modeling: Application and validation of GEOSPACE-1D, https://doi.org/10.5281/zenodo.19773216, 2026.

David, O., Ascough, J. C., Lloyd, W., Green, T. R., Rojas, K. W., Leavesley, G. H., and Ahuja, L. R.: A software engineering perspective on environmental modeling framework design: The Object Modeling System, Environmental Modelling & Software, 39, 201–213, 2013.

de Pury, D. G. G. and Farquhar, G. D.: Simple scaling of photosynthesis from leaves to canopies without the errors of big-leaf models, Plant Cell Environ., 20, 537–557, 1997.

Dubbert, M. and Werner, C.: Water fluxes mediated by vegetation: emerging isotopic insights at the soil and atmosphere interfaces, New Phytol., 221, 1754–1763, https://doi.org/10.1111/nph.15547, 2019.

Fatichi, S., Ivanov, V. Y., and Caporali, E.: A mechanistic ecohydrological model to investigate complex interactions in cold and warm water-controlled environments: 1. Theoretical framework and plot-scale analysis, J. Adv. Model. Earth Syst., 4, https://doi.org/10.1029/2011ms000086, 2012.

Formetta, G., Antonello, A., Franceschi, S., David, O., and Rigon, R.: Hydrological modelling with components: A GIS-based open-source framework, Environmental Modelling & Software, 55, 190–200, 2014.

Freyberg, J., Allen, S. T., Grossiord, C., and Dawson, T. E.: Plant and root-zone water isotopes are difficult to measure, explain, and predict: Some practical recommendations for determining plant water sources, Methods Ecol. Evol., 11, 1352–1367, https://doi.org/10.1111/2041-210x.13461, 2020.

Frédette, C., Labrecque, M., Comeau, Y., and Brisson, J.: Willows for environmental projects: A literature review of results on evapotranspiration rate and its driving factors across the genus Salix, J. Environ. Manage., 246, 526–537, https://doi.org/10.1016/j.jenvman.2019.06.010, 2019.

Gamma, E., Helm, R., Johnson, R., . Johnson, R. E., and Vlissides, J.: Design Patterns: Elements of Reusable Object-Oriented Software, Pearson Deutschland GmbH, 1995.

Grant, G. E. and Dietrich, W. E.: The frontier beneath our feet, Water Resources Research, 53, 2605–2609, 2017.

Guidi, W., Piccioni, E., and Bonari, E.: Evapotranspiration and crop coefficient of poplar and willow short-rotation coppice used as vegetation filter, Bioresour. Technol., 99, 4832–4840, https://doi.org/10.1016/j.biortech.2007.09.055, 2008.

Guswa, A. J., Tetzlaff, D., Selker, J. S., Carlyle-Moses, D. E., Boyer, E. W., Bruen, M., Cayuela, C., Creed, I. F., Giesen, N., Grasso, D., Hannah, D. M., Hudson, J. E., Hudson, S. A., Iida, S., Jackson, R. B., Katul, G. G., Kumagai, T., Llorens, P., Lopes Ribeiro, F., Michalzik, B., Nanko, K., Oster, C., Pataki, D. E., Peters, C. A., Rinaldo, A., Sanchez Carretero, D., Trifunovic, B., Zalewski, M., Haagsma, M., and Levia, D. F.: Advancing ecohydrology in the 21st century: A convergence of opportunities, Ecohydrol., 13, 1, 2020.

Hargreaves, G. H.: Accuracy of Estimated Reference Crop Evapotranspiration, J. Irrig. Drain Eng., 115, 1000–1007, https://doi.org/10.1061/(ASCE)0733-9437(1989)115:6(1000), 1989.

Heinsoo, K., Koppel, A., and Merilo, E.: Estimation of leaf area index in a willow plantation, Proc. Estonian Acad. Sci. Biol. Ecol., 53, 3, 2004.

Jarvis, P. G., Monteith, J. L., and Weatherley, P. E.: The interpretation of the variations in leaf water potential and stomatal conductance found in canopies in the field, Philos. Trans. R. Soc. Lond. B Biol. Sci., 273, 593–610, 1976.

Kuppel, S., Tetzlaff, D., Maneta, M. P., and Soulsby, C.: EcH $_2$O-iso 1.0: water isotopes and age tracking in a process-based, distributed ecohydrological model, Geosci. Model Dev., 11, 3045–3069, https://doi.org/10.5194/gmd-11-3045-2018, 2018.

Macfarlane, C., White, D. A., and Adams, M. A.: The apparent feed-forward response to vapour pressure deficit of stomata in droughted, field-grown Eucalyptus globulus Labill, Plant Cell Environ., 27, 1268–1280, 2004.

Merilo, E., Heinsoo, K., Kull, O., Söderbergh, I., and Koppel, A.: Leaf photosynthetic properties in a willow (Salix viminalis and Salix dasyclados) plantation in response to fertilization, Eur. J. For. Res., 125, 93–100, 2006.

National Research Council, Commission on Geosciences, Environment, and Resources, Board on Earth Sciences and Resources, and Committee on Basic Research Opportunities in the Earth Sciences: Basic Research Opportunities in Earth Science, National Academies Press, 2001.

Nehemy, M. F., Benettin, P., Asadollahi, M., Pratt, D., Rinaldo, A., and McDonnell, J. J.: Dataset: The SPIKE II experiment - Tracing the water balance, https://doi.org/10.5281/zenodo.4037240, 2020.

https://doi.org/10.5194/egusphere-2026-2385
Preprint. Discussion started: 28 July 2026

Nehemy, M. F., Benettin, P., Asadollahi, M., Pratt, D., Rinaldo, A., and McDonnell, J. J.: Tree water deficit and dynamic source water partitioning, Hydrol. Process., 35, 2021.

Penman, H. L. and Keen, B. A.: Natural evaporation from open water, bare soil and grass, Proc. R. Soc. Lond. A Math. Phys. Sci., 193, 120–145, 1948.

Peters, A., Groh, J., Schrader, F., Durner, W., Vereecken, H., and Pütz, T.: Towards an unbiased filter routine to determine precipitation and evapotranspiration from high precision lysimeter measurements, Journal of Hydrology, 549, 731–740, https://doi.org/10.1016/j.jhydrol.2017.04.015, 2017.

Porporato, A. and Yin, J.: Ecohydrology: Dynamics of life and water in the critical zone, Cambridge University Press, Cambridge, England, https://doi.org/10.1017/9781108886321, 2022.

Priestley, C. H. B. and Taylor, R. J.: On the Assessment of Surface Heat Flux and Evaporation Using Large-Scale Parameters, Mon. Weather Rev., 100, 81–92, 1972.

Rigon, R., Formetta, G., Bancheri, M., Tubini, N., D'Amato, C., David, O., and Massari, C.: HESS Opinions: Participatory Digital eARth Twin Hydrology systems (DARTHs) for everyone – a blueprint for hydrologists, Hydrol. Earth Syst. Sci., 26, 4773–4800, 2022.

Rinaldo, A.: Ecohydrology amid a rapidly changing world, Nat. Water, 2, 209–210, https://doi.org/10.1038/s44221-024-00205-w, 2024.

Rinaldo, A. and Rodriguez-Iturbe, I.: Ecohydrology 2.0, Rend. Lincei Sci. Fis. Nat., 33, 245–270, https://doi.org/10.1007/s12210-022-01071-y, 2022.

Rodriguez-Iturbe, I.: Ecohydrology: A hydrologic perspective of climate-soil-vegetation dynamics, Water Resources Research, 36, 2000.

Simunek, J., Van Genuchten, M. T., and Sejna, M.: The HYDRUS-1D software package for simulating the one-dimensional movement of water, heat, and multiple solutes in variably-saturated media, University of California-Riverside Research Reports, 3, 1–240, 2005.

Sinclair, T. R. and Ludlow, M. M.: Influence of soil water supply on the plant water balance of four tropical grain legumes, Australian Journal of Plant Physiology, 13, 329–341, https://doi.org/10.1071/PP9860329, 1986.

Smettem, K. R. J.: Welcome address for the new 'Ecohydrology' Journal, Ecohydrology, 1, 1–2, 2008.

Smith, M. D., Sikka, A., Taguta, C., Dirwai, T. L., and Mabhaudhi, T.: Embracing complexities in agricultural water management through nexus planning, Irrig. Drain., 2024.

Sprenger, M., Leistert, H., Gimbel, K., and Weiler, M.: Illuminating hydrological processes at the soil-vegetation-atmosphere interface with water stable isotopes, Rev. Geophys., 54, 674–704, https://doi.org/10.1002/2015rg000515, 2016.

Tubini, N.: Theoretical and numerical tools for studying the Critical Zone from plot to catchments, Ph.D. thesis, University of Trento, 2021.

Tubini, N. and Rigon, R.: Implementing the Water, HEat and Transport model in GEOframe (WHETGEO-1D v.1.0): algorithms, informatics, design patterns, open science features, and 1D deployment, Geosci. Model Dev., 15, 75–104, 2022.

White, D. A., Beadle, C. L., Sands, P. J., Worledge, D., and Honeysett, J. L.: Quantifying the effect of cumulative water stress on stomatal conductance of Eucalyptus globulus and Eucalyptus nitens: A phenomenological approach, Aust. J. Plant Physiol., 26, 17–27, 1999.

Wilkinson, M. D., Dumontier, M., Aalbersberg, I. J. J., Appleton, G., Axton, M., Baak, A., Blomberg, N., Boiten, J.-W., da Silva Santos, L. B., Bourne, P. E., Bouwman, J., Brookes, A. J., Clark, T., Crosas, M., Dillo, I., Dumon, O., Edmunds, S., Evelo, C. T., Finkers, R., Gonzalez-Beltran, A., Gray, A. J. G., Groth, P., Goble, C., Grethe, J. S., Heringa, J., 't Hoen, P. A. C., Hooft, R., Kuhn, T., Kok, R., Kok, J., Lusher, S. J., Martone, M. E., Mons, A., Packer, A. L., Persson, B., Rocca-Serra, P., Roos, M., van Schaik, R., Sansone, S.-A., Schultes, E., Sengstag, T., Slater, T., Strawn, G., Swertz, M. A., Thompson, M., van der Lei, J., van Mulligen, E., Velterop, J., Waagmeester, A., Wittenburg, P., Wolstencroft, K., Zhao, J., and Mons, B.: The FAIR Guiding Principles for scientific data management and stewardship, Sci Data, 3, 160018, 2016.